

Stirring Effect on the Belousov-Zhabotinsky Oscillating Chemical Reactions in a Batch. Experimental and Modelling

Yevhen Yu. Kalishyn^a, Małgorzata Rachwalska^b, and Peter E. Strizhak^a

^a L. V. Pysarzhevsky Institute of Physical Chemistry of National Academy of Sciences of Ukraine, pr.Nauky 31, Kyiv, 03039, Ukraine

^b Faculty of Chemistry, Jagiellonian University, ul.Ingardena 3, 30-060 Kraków, Poland

Reprint requests to Dr. M. R.; Fax: +48-12-6340515; E-mail: rachwals@chemia.uj.edu.pl

Z. Naturforsch. **65a**, 132–140 (2010); received March 3, 2008 / revised July 30, 2009

We have studied the stirring effect on the time-delayed bifurcations of transient oscillations in the Belousov-Zhabotinsky (BZ) oscillating chemical reaction in a closed system. Experiments show that oscillations disappear through the time-delayed Hopf bifurcations, whose parameters depend on the stirring rate. The explanation of the stirring effect is based on the theories of diffusion-controlled reactions and hydrodynamic turbulence. We show that an increase of the stirring rate leads to an increase of the rate constant for the diffusion-controlled reaction. We propose a kinetic scheme that describes the effect observed in the experiments. A good agreement between the experimental data and the simulations is obtained.

Key words: Stirring Effect; Diffusion-Controlled Reactions.

1. Introduction

The stirring effects in nonlinear chemical reactions have been studied for a long time. On the one hand an explanation of the stirring effect leads to an understanding, that the efficiency of mixing is a key factor for nonlinear chemical systems and, on the other hand, the stirring rate of the reaction volume must be considered as a bifurcation parameter.

The stirring effect has been observed in various oscillating systems. Among them there are the chlorite-iodide reaction, the minimal bromate oscillators [1, 2], the $\text{IO}_3^-/\text{H}_3\text{AsO}_3$ reaction [3], and the Belousov-Zhabotinsky (BZ) reaction [4].

The stirring rate may change the dynamic behaviour of a system in a quantitative or in a qualitative manner, as well. Quantitative stirring effects refer to changes in rates, steady-state concentrations, parameters of regular oscillations, and positions of bifurcations points. Qualitative effects are, e. g., inhomogeneity-induced oscillations, formation of mushroom and isola, and transitions between periodic and aperiodic oscillations.

The stirring effects were interpreted in the framework of macromixing or micromixing concepts. The consideration via macromixing models is based on the assumption of the macroscopic spatial concentration gradients which exist, whereas micromixing

approaches consider only the microscale eddies arising in the cascade of turbulent energy dissipation. A classification of stirring effects, due to incomplete mixing of feedstreams, was established recently in terms of a simple coupled reactor model (macromixing). Stirring effects may be also associated with differential-flow-induced chemical instability, discovered recently.

Moreover, the dynamic behaviour of nonlinear chemical systems in a continuous stirred tank reactor (CSTR) shows also the behavioural dependence on the mixing mode: mixing the reactants prior to entering the reactor (premixed mode) or separately pumping the reactants into the CSTR (nonpremixed mode).

The BZ oscillating chemical reaction is the most important in modern chemistry. To understand the key mechanisms of the BZ reaction, it is necessary to know how stirring rates affect the BZ reaction. It has been shown that stirring rates may affect the oscillating dynamics in the BZ reaction catalyzed by various compounds: cerium, manganese, and ferroin. Moreover, the BZ reaction can be performed in a CSTR and in a batch.

The stirring effect on the BZ reaction in a CSTR has been most thoroughly studied. In addition, stirring-induced transitions from periodic to aperiodic oscillations have been reported for a BZ system in a CSTR. The scatter of the largest Lyapunov exponents and of

the correlation dimensions for a chaotic regime in the BZ reaction has been found to decrease with increasing stirring rate in a CSTR. It has also been found that irregular oscillations in a closed anerobic BZ system, occurring at slow stirring rates, might be associated with excitations induced by fluctuations. Furthermore, low stirring rates and high temperature increases the oscillating frequency and decreases the amplitude in the BZ reaction catalyzed by ferroin if gallic acid is the substrate [5].

It is important to remark that atmospheric oxygen has a strong effect on the reaction whenever the BZ reaction is studied in a reactor open to the atmosphere. In fact, a few years ago all stirring effects were thought to be caused by atmospheric oxygen [6]. However, more recently the effect of stirring has been observed in an inert atmosphere [7].

Mostly, the studies of stirring rates on the BZ reaction in batch were developed by varied stirring rates in time series. It was found that the effects of stirring definitely depend on the initial concentrations of reagents in the BZ reaction. Namely, the maximum global stirring sensitivity is observed when the BZ reaction is conducted with low concentrations of malonic acid [8]. Moreover, it was shown that an increased stirring rate increases both the induction and oscillating period. The results give an indication of the qualitative role of stirring and of temperature as bifurcation parameters in a Hopf bifurcation experiment [9]. It was observed that the frequency of the oscillations increases as the stirring rate decreases. At high stirring rates (ca. 900 rpm) the system settles into a reduced non-oscillatory (excitable) steady state. When the stirring rate is reduced to 300 rpm, oscillations reappear immediately (stirring-induced excitation) [10].

Different stirring effects for the Belousov-Zhabotinsky (BZ) reaction can be explained by macromixing or micromixing concepts. Moreover, it is important to consider that the rate of the diffusion-controlled step depends upon the stirring rate [11].

In this paper we present a study of the stirring effect on the transient regimes in the BZ reaction catalyzed by ferroin in a batch. Our experiments show that the stirring rate controls the time-dependent Hopf bifurcation of transient regimes. We suggest explanations of the stirring effect based on the theories of diffusion-controlled reactions and hydrodynamic turbulence. We propose a kinetic scheme that describes the effects observed in experiments. We show that an increase of the stirring rate leads to an increase of the rate constant

of diffusion-controlled reactions. Good agreement between the simulations and the experimental results is obtained.

2. Experimental

2.1. Reagents

Analytical grade chemicals KBrO_3 , H_2SO_4 , 1,10-phenanthroline ("POCH" S. A. Gliwice) and malonic acid (Aldrich) were used without further purification. Stock solutions of KBrO_3 , H_2SO_4 , and malonic acid were prepared using double distilled water. Aqueous ferroin solution was prepared using a standard method [12].

2.2. Apparatus

A cylindrical glass vessel (diameter 37 mm, height 110 mm) was used in all experiments. The reactor and the glass vessel were maintained at 24.5 °C. The stirring rate was varied between 100 and 900 rpm. A rod shaped teflon coated magnetic stirrer (length 25 mm, diameter 5 mm) was applied. The volume of the reaction mixture was 40 ml. The state of the system was monitored by measuring the platinum electrode potential using a saturated calomel reference electrode connected with the reaction mixture by a salt bridge with 1 M KNO_3 . Changes of the potentials over time were recorded by MTA (Kutesz type 1040/4) recorder and by PC computer. Signals were recorded as a function of time with a time step of 0.1s. The time series were recorded until the oscillations ceased.

2.3. Procedures

In our batch experiments the reaction was initiated by adding the ferroin solution into the mixture of KBrO_3 , MA, and H_2SO_4 . In all experiments the initial concentrations of reagents were fixed: $[\text{KBrO}_3]_0 = 0.19 \text{ M}$, $[\text{MA}]_0 = 0.68 \text{ M}$, $[\text{H}_2\text{SO}_4]_0 = 0.32 \text{ M}$, $[\text{ferroine}]_0 = 0.00338 \text{ M}$. Each time series corresponds to a separate value of stirring rate. Before adding the ferroin solution into the reaction mixture, argon gas was passed over the reaction mixture at a velocity of 100 l/h for approximately 30 min in order to stabilize the atmosphere in the reactor. We maintained the reaction mixture at 24.5 °C not only during the measurement but also in the first 30 min when stabilizing the atmosphere in the reactor. Hence, the small amount of dissolved oxygen might have been removed from

the solution in the conditions of mixing. It is so because the higher temperature and mixing well remove the dissolved gaseous. All experiments were performed while flowing argon over the reaction mixture in order to eliminate any effects of oxygen in an experimental set up described by us in [13].

3. Experimental Results

The very beginning of the experimental result for stirring rate 100 rpm is presented in Figure 1. One can see that oscillations start after ca. 40 s from the time of mixing up the reagents and that they have a mixed mode character. Then the oscillations get the L type. The time dependence of the Pt-electrode potential is shown in Figure 2a for the BZ reaction running at the stirring rate of 100 rpm. Correspondingly, Figure 2c and 2e represent the time dependence of the amplitude and the period of oscillations. Figure 2c shows that the amplitude of the oscillations decreases in time. The disappearance of oscillations is characterized by their diminishing amplitude which are close to zero

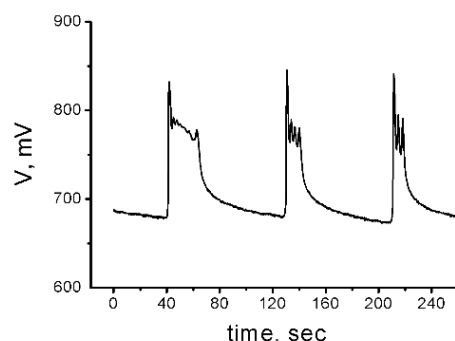


Fig. 1. Very beginning of the experimental run presented in Figure 2a.

(Fig. 2c). The time dependence of the oscillation periods is characterized by a volcano shape curve as illustrated by Figure 2e. Analysis of this figure shows that the oscillations disappear at a non-zero value of the period. A similar result was found for the time dependence of the Pt-electrode potential, the amplitude and period of oscillations observed at stirring rates between 100 and 900 rpm. The experimental dependence

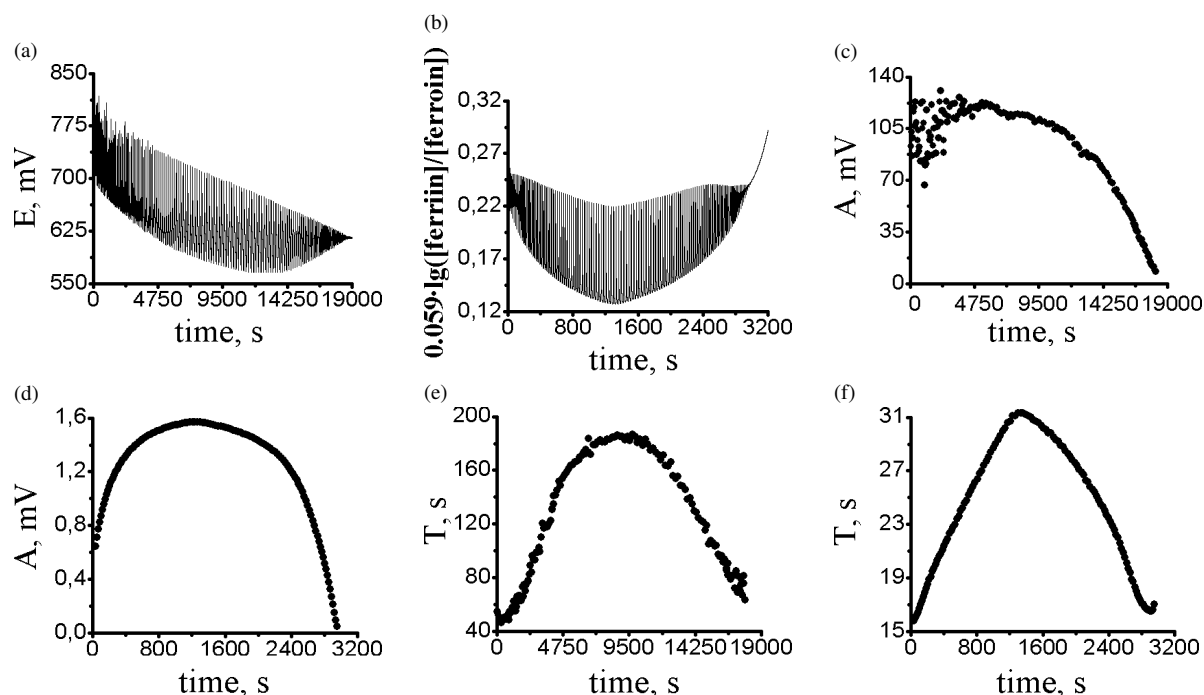


Fig. 2. Oscillations of the Pt-electrode potential (a), their amplitude (c), and their period (e) as functions of time for a closed BZ system (initial concentrations: $[\text{KBrO}_3]_0 = 0.19 \text{ M}$, $[\text{H}_2\text{SO}_4]_0 = 0.32 \text{ M}$, $[\text{MA}]_0 = 0.68 \text{ M}$; $[\text{ferroin}]_0 = 3.38 \cdot 10^{-3} \text{ M}$); the stirring rate is 100 rpm. Oscillations of $\lg \frac{[\text{ferrin}]}{[\text{ferroin}]}$ (b), their amplitude (d) and their period (f) as functions of time obtained in numerical simulations using the model presented in Table 1 (initial concentrations: $[\text{KBrO}_3]_0 = 0.19 \text{ M}$, $[\text{Br}^-]_0 = 10^{-7} \text{ M}$, $[\text{MA}]_0 = 0.05 \text{ M}$; $[\text{ferroin}]_0 = 3.38 \cdot 10^{-3} \text{ M}$, $[\text{H}^+] = 0.44 \text{ M}$, and zero concentrations for other components; the stirring rate is 100 rpm)

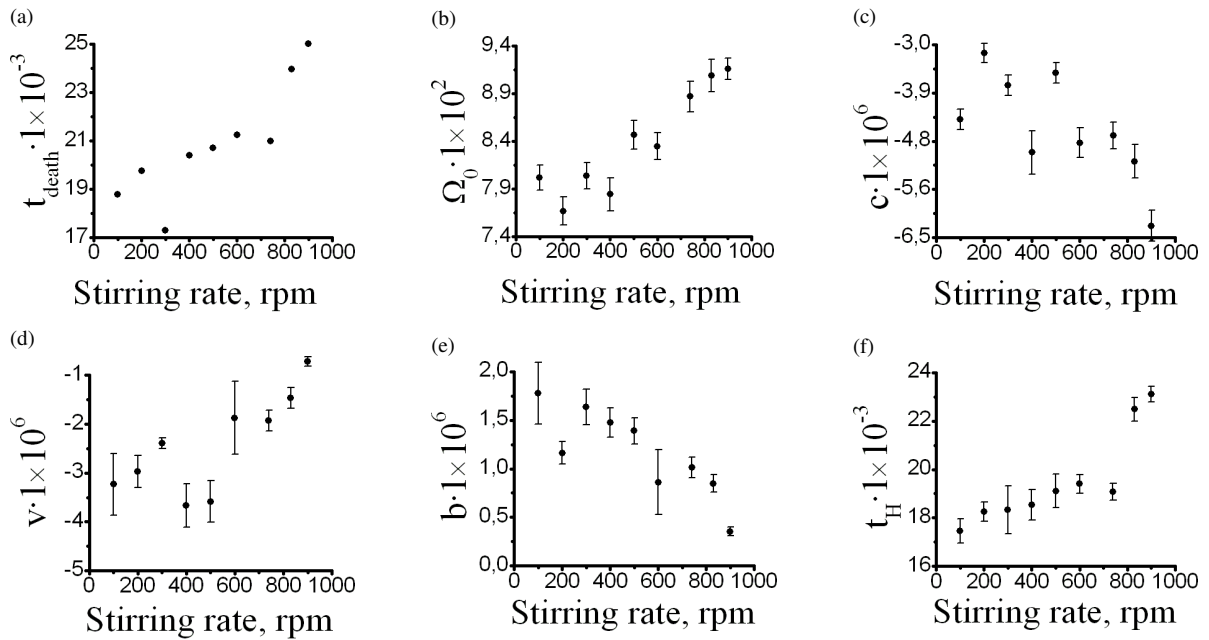


Fig. 3. Dependencies of extinction time of oscillations (a) taken from the experimental data and parameters of equations (1), (2), and (7) (b–f) on stirring rate obtained by the analysis of experimental results. Conditions are the same as in Figure 1.

of the oscillations' time of death (t_{death}) on the stirring rate is shown in Figure 3a. Analysis of this figure shows that the oscillations' time of death value increases with increased stirring rate.

The qualitative behaviour of time dependences allows us to make the following conclusion. At the various stirring rates the oscillations decay through the time-delayed Hopf bifurcation. Figures 3 and 4 show data determined from both experiment and calculation. The experimental and calculated errors are indicated by horizontal bars. One should mention that those errors show an accuracy of period estimation obtained in experiments and its influence on position of calculated values obtained in model simulation. We should mention that the following values should also be taken into account in signed values of errors: (i) accuracy of initial concentrations estimation and (ii) stability of the argon flow rate. Because of the difficulty of the task, we have not taken into account (i) and (ii).

3.1. The Time-Delayed Hopf Bifurcation [14, 15, 16]

Scalings between characteristics for the time-delayed Hopf bifurcation and the stirring rate are represented by Figures 3b–f. These scalings were calculated from experimental results. Figures 3b and 3c

show the dependence of the frequency of oscillations at the death time of oscillations (Ω_0) and the rate of change of the oscillation amplitude (c) on the stirring rate. The dependence of both Ω_0 and c on time is described by the following equation:

$$\Omega(t) = \Omega_0 + c \cdot A^2(t), \quad (1)$$

where A is the amplitude of oscillations and Ω the frequency of oscillation. The linear rate of the control parameter change (v), the linear rate of the change of the amplitude near the Hopf point (b), the time of real Hopf bifurcation (t_H) vs. the stirring rate are shown in Figures 3d, 3e, and 3f, respectively. The scaling is described by the following equation:

$$A^2 = [v \cdot (t - t_H)]/b. \quad (2)$$

Scalings calculated from simulation are represented by Figures 4b–f.

Figure 4b shows that the value of Ω_0 increases with increasing stirring rate. The parameter c (Fig. 3c) is not monotonic. In general the value of c decreases if the stirring rate increases. An increasing stirring rate leads to an increasing parameter v and decreasing parameter b as illustrated in Figures 4d and 4e, respectively. Contrary to Figure 4e, the time of the real Hopf

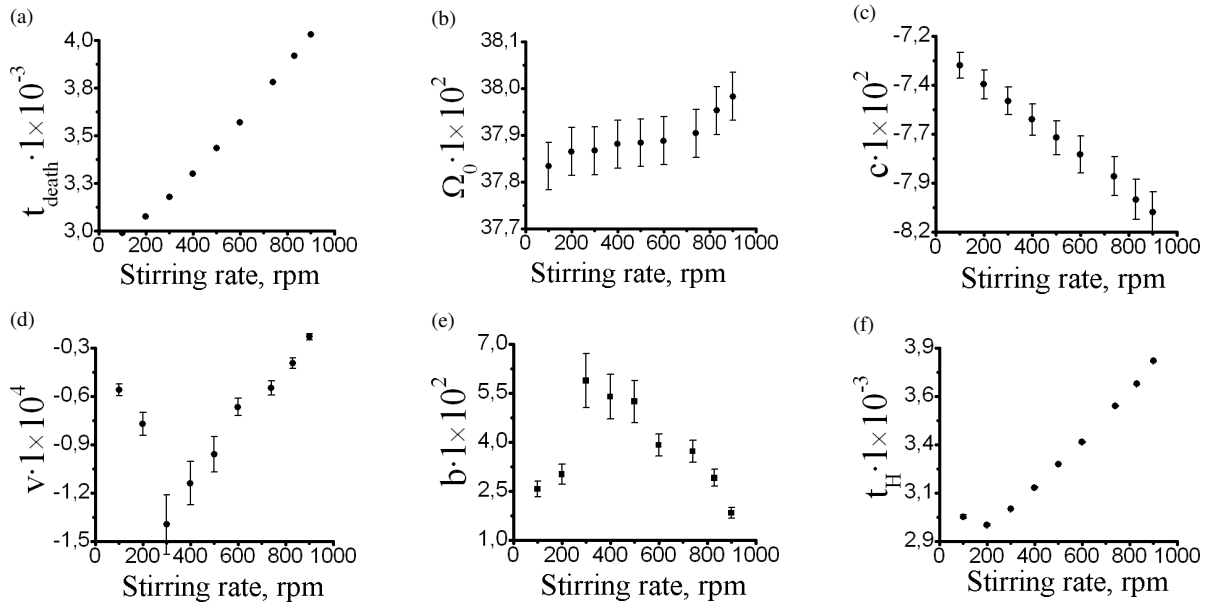


Fig. 4. Dependencies of extinction time of oscillations obtained by the numerical simulations of the kinetic scheme presented in Table 1 (a) and parameters of equations (1), (2), and (7) (b–f) vs. stirring rate. Conditions are the same as in Figure 1.

bifurcation (t_H) grows with an increasing stirring rate (Fig. 4f). These dependences are in agreement with the results predicted by Figure 3c. Note that decreasing the value c should increase the value of t_H and vice versa.

4. Analysis and Simulations

Our explanation of the stirring effect is based on the theories of diffusion controlled reactions and hydrodynamic turbulence.

The rate constant k_D for a diffusion-controlled reaction is

$$k_D = 4\pi N_A \cdot D_{\text{EFF}} \cdot d \quad [17], \quad (3)$$

where N_A is the Avogadro's constant, D_{EFF} the effective diffusion coefficient, d the average distance between the reactive species [11].

It is

$$D_{\text{EFF}} = D_{\text{MOL}} + D_{\text{TURB}}, \quad (4)$$

where D_{MOL} is the molecular diffusion coefficient ($\approx 10^{-5} \text{ cm}^2 \text{ s}^{-1}$) and D_{TURB} the turbulent diffusion coefficient. D_{TURB} is given by [11, 18, 19]

$$D_{\text{TURB}} = d^2 \cdot S^{3/2} \cdot \lambda \cdot \eta^{-1/2}, \quad (5)$$

where $S = 2\pi \cdot$ stirring rate (the stirring rate is in a variable range of 100–900 rpm, in our case). λ is

the stirrer radius ($\approx 1.25 \text{ cm}$) and η is the kinematic viscosity ($\approx 1 \cdot 10^{-2} \text{ cm}^2 \text{ s}^{-1}$). We have estimated d as $\approx 0.13 \cdot 10^{-6} \text{ cm}$ but in reality we have used as d the value $3 \cdot 10^{-6} \text{ cm}$. For simulation we used the following initial concentration of reagents: $(0.19 + 0.05 + 0.003 + 0.44 = 0.7) \text{ M}$. We have obtained ca. $0.13 \cdot 10^{-6} \text{ cm}$ as the distance between particles in this case in the following way:

We have $0.7 \cdot 6 \cdot 10^{23}$ particles in 1000 ml. Hence, we can easily calculate that one particle is in the volume of $1000 / (4.2 \cdot 10^{23}) \text{ cm}^3 = 0.24 \cdot 10^{-20} \text{ cm}^3$, i.e. in our solution there is one particle in a cube whose edge is ca. $0.13 \cdot 10^{-6} \text{ cm}$. So the reaction partners are separated by a distance of ca. $1.3 \cdot 10^{-7} \text{ cm}$. In order to describe well our experimental results we have to assume $3 \cdot 10^{-6} \text{ cm}$ as the distance between particles. It shows that the distance is greater than the calculated $0.13 \cdot 10^{-6} \text{ cm}$ and it could be real because in reaction R10 not all reagents take part. Therefore, the distance between them should be greater than calculated for the situation of initial conditions. According to equations (3)–(5), the rate constant of the diffusion controlled reaction R10 can be expressed as:

$$k_{10} = k_{10,S=0} + 4\pi N_D \cdot d^3 \cdot S^{3/2} \cdot \lambda \cdot \eta^{-1/2}, \quad (6)$$

where $k_{10,S=0} = 2 \cdot 10^9 \text{ M}^{-1} \text{ s}^{-1}$.

No	Chemical reactions	Experimental rate constant	Ref. no
R1	$\text{BrO}_3^- + \text{Br}^- + 2\text{H}^+ \xrightarrow{k_1} \text{HBrO}_2 + \text{HOBr}$	$2 \cdot [\text{H}^+]^2 \text{ M}^{-1} \text{ s}^{-1}$	[20–23]
R2	$\text{HBrO}_2 + \text{Br}^- + \text{H}^+ \xrightarrow{k_2} 2\text{HOBr}$	$2 \cdot 10^6 \cdot [\text{H}^+] \text{ M}^{-1} \text{ s}^{-1}$	[20, 21, 23]
R3	$\text{BrO}_3^- + \text{HBrO}_2 + \text{H}^+ \xrightarrow{k_3} 2\text{BrO}_2^\bullet + \text{H}_2\text{O}$	$50 \cdot [\text{H}^+] \text{ M}^{-1} \text{ s}^{-1}$	[20, 23, 24]
R4	$2\text{BrO}_2^\bullet + \text{H}_2\text{O} \xrightarrow{k_4} \text{BrO}_3^- + \text{HBrO}_2 + \text{H}^+$	$4.2 \cdot 10^7 \text{ M}^{-1} \text{ s}^{-1}$	[20, 23, 24]
R5	$\text{BrO}_2^\bullet + \text{Fe}(\text{phen})_3^{2+} + \text{H}^+ \xrightarrow{k_5} \text{HBrO}_2 + \text{Fe}(\text{phen})_3^{3+}$	$1 \cdot 10^9 [\text{H}^+] \text{ M}^{-1} \text{ s}^{-1}$	[22, 24]
R6	$\text{HBrO}_2 + \text{Fe}(\text{phen})_3^{3+} \xrightarrow{k_6} \text{BrO}_2^\bullet + \text{Fe}(\text{phen})_3^{2+} + \text{H}^+$	$40 \text{ M}^{-1} \text{ s}^{-1}$	[20, 22, 24]
R7	$2\text{HBrO}_2 \xrightarrow{k_7} \text{BrO}_3^- + \text{HOBr}$	$3000 \text{ M}^{-1} \text{ s}^{-1}$	[20, 21]
R8	$\text{MA} + \text{HOBr} \xrightarrow{k_8} \text{BrMA}$	$8.2 \text{ M}^{-1} \text{ s}^{-1}$	[20, 21]
R9	$\text{BrMA} + \text{Fe}(\text{phen})_3^{3+} \xrightarrow{k_9} \text{BrMA}^\bullet + \text{Fe}(\text{phen})_3^{2+} + \text{H}^+$	$20 \text{ M}^{-1} \text{ s}^{-1}$	[20, 21, 25]
R10	$\text{BrMA}^\bullet + \text{Fe}(\text{phen})_3^{3+} + \text{H}^+ \xrightarrow{k_{10}} \text{BrMA} + \text{Fe}(\text{phen})_3^{3+}$	$2 \cdot 10^9 [\text{H}^+] \text{ M}^{-1} \text{ s}^{-1}$	[20]
R11	$\text{BrMA}^\bullet \xrightarrow{k_{11}} \text{Br}^-$	7 s^{-1}	[26, 27]
R12	$2\text{BrMA}^\bullet \xrightarrow{k_{12}} \text{BrTTA} + \text{BrMA}$	$1 \cdot 10^8 \text{ M}^{-1} \text{ s}^{-1}$	[21]
R13	$\text{BrTTA} \xrightarrow{k_{13}} \text{Br}^- + \text{MOA} + \text{H}^+$	1.5 s^{-1}	[28]
R14	$\text{Fe}(\text{phen})_3^{2+} \xrightarrow{k_{14}} \text{products}$	$7.5 \cdot 10^{-5} \text{ s}^{-1}$	[23]

Table 1. Kinetic scheme describing the stirring effect on transient regimes in the BZ reaction catalyzed by ferroin.

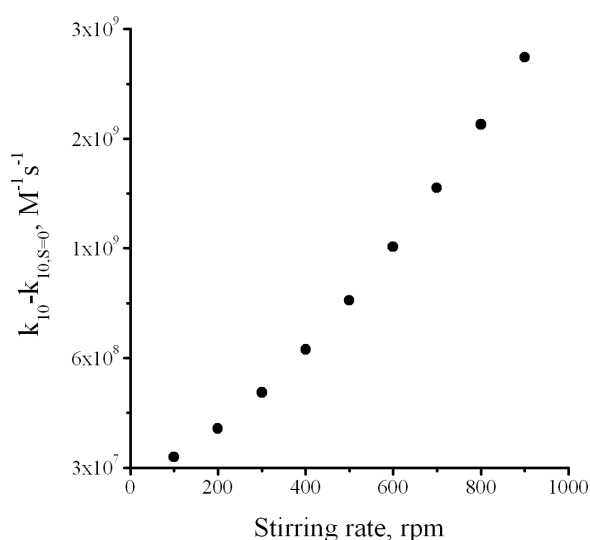


Fig. 5. Dependence of $k_{10} - k_{10,S=0}$, i. e. the rate constant of diffusion-controlled reaction (k_D) on the stirring rate obtained from Equation (6).

The dependence of $(k_0 - k_{10,S=0})$ on the stirring rate is shown on Figure 5.

4.1. The Model

To describe the stirring effect we propose the kinetic scheme presented in Table 1. The kinetic scheme consists of 14 elementary reactions for 10 kinetic variables. Reactions R1–R7 describe interactions between bromine-containing compounds. Reaction R8 describes the formation of brommalonic acid (BrMA). It produces BrMA^\bullet according to the reaction R9. The

reactions R10, R11, and R12 describe the consumption of BrMA^\bullet . The Br^- production is described by reactions R11 and R13. The reaction of MA with HOBr (R8) was written to occur directly, not via the enolized form. Replacing reaction R8 by the corresponding enol reaction has no influence on the dynamic behaviour of the system.

Our simulations have shown that reactions R1–R13 describe oscillations that last more than 300 h. Adding the reaction R14, describing the degradation of the catalyst, decreases the oscillation lifetime.

Kinetic equations were written in accordance with the mass action law. We analyzed the time dependencies of $\lg \frac{\text{ferriin}}{\text{ferroin}}$ corresponding to the platinum electrode potential.

The reaction R10 between ferroin and BrMA^\bullet was chosen as the diffusion controlled reaction. Numerical simulations of the stirring effect were taken into account by introducing the rate constant of reaction R10, according to equation (6), into the kinetic scheme in Table 1. As initial concentrations we used the following values:

$$[\text{KBrO}_3]_0 = 0.19 \text{ M}, \quad [\text{MA}]_0 = 0.05 \text{ M}, \\ [\text{H}^+]_0 = 0.44 \text{ M}, \quad [\text{ferroin}]_0 = 0.00338 \text{ M}.$$

4.2. Simulation Results

The theoretical time dependence of $\lg \frac{\text{ferriin}}{\text{ferroin}}$ is shown in Figure 2b for a stirring rate of 100 rpm. Correspondingly, Figures 2d and 2f represent the time dependences of the amplitude and the period of oscillations.

tions. The amplitude and the period of oscillations are characterized by the volcano shaped curves. Changing the stirring rate within the range of 100 to 900 rpm, for the kinetic scheme, gives the same dependencies of amplitude and oscillations' period as illustrated by Figures 2d–2f. Numerical simulations show that the value of t_d , (death's time of oscillations) increases with increasing stirring rate as illustrated by Figure 4a.

Figures 4b–f illustrate the dependencies between the parameters for the time-delayed Hopf bifurcation and the stirring rate calculated for the numerical simulation. The value of Ω_0 increases with increasing stirring rate (Figure 4b).

Values of c and b decrease with increasing stirring rate (Figs. 4c and 4e). Contrarily, values of v and t_H increase if the stirring rate increases as illustrated by Figures 4d and 4f.

5. Discussion

Our studies indicate that the oscillations disappear with the non-zero value of the period and the zero value of the amplitude at various stirring rates (Figs. 2c, e). Moreover the oscillations continue longer with increasing stirring rate. Such dependencies of amplitude and period with time led us to conclude that oscillations undergo the time-delayed Hopf bifurcation.

To describe the stirring effect a chemically realistic model was suggested. Our kinetic scheme consists of: (i) inorganic oxybromine chemical reactions leading to the removal of the inhibitor bromide and to the accumulation of bromine containing compounds (HOBr, HBrO₂, BrO₂); (ii) reactions with catalysts, and reactions between organic species that lead to the accumulation of bromide ions.

Now some words on how we construct the proposed kinetic scheme. We take the full kinetic scheme that may describe various regimes in the BZ reaction catalyzed by ferroin. Next we take away step by step the chemical reactions from the kinetic scheme and we check how kinetic scheme may describe the stirring effect. Finally, we get a minimal set of chemical reactions that describe the stirring effect on the BZ reaction catalyzed by ferroin. Our results of simulation agree with experimental data.

It should be noticed that our earlier results show that the proposed kinetic scheme may describe also an oxygen effect on the BZ reaction catalyzed by ferroin [13]. Results of the simulation of oxygen and stirring rate show that the proposed kinetic scheme

includes sufficiently a set of chemical reactions that may describe these effects. This was our main goal for the simulation.

If we include for example the reaction



into the reactions' set, oscillations fail, but it is possible to get again oscillations when changing a little only one of initial the concentrations. Hence we determine a number of chemical reactions engaged in the description of some experimental results with certain preciseness.

The analysis of the data presented in Figures 2a, c, e and Figures 2b, d, f indicates a likely correspondence between experimental results and simulations.

5.1. Stirring Effect and Other Rate Constants (Connected with Reaction R5)

In the suggested model there are two diffusion-controlled reactions. There are reactions between BrMA• and ferroin (R10), and between bromine dioxide and ferroin (R5). The effect of reaction R10 has been discussed above. Reaction R5 is fast but somewhat slower than the mentioned above diffusion controlled reaction. Moreover, we have performed numerical simulations by varying the rate constant of reaction R5. It was shown that increasing the value of k_5 decreases the time of existence of the oscillations. Such behaviour, however, is contrary to the experimental behaviour. Therefore, it is concluded that the reaction R5 cannot be responsible for the observed stirring effects.

5.2. Stochastic method

Stirring effects on the nonlinear dynamics were considered mostly in terms of stochastic noise. Numerical simulations take into account the random noise in the differential equation which describes the stirring effects. Experimental results, reported above, have shown that the oscillations disappear, via the time-delayed Hopf bifurcation, at various values of the stirring rate. We have developed numerical simulations of the stirring effect on the normal form of Hopf bifurcation. In this case the equations for the oscillation amplitude can be written in the following form:

$$\frac{dA}{dt} = [v \cdot (t - t_H) - bA^2] \cdot A; \quad (7)$$

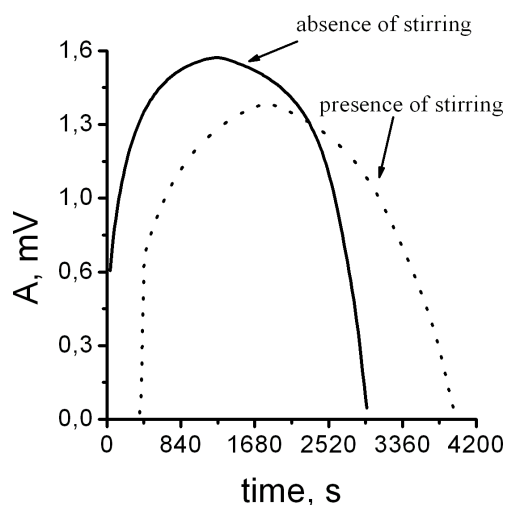


Fig. 6. Dependence of oscillations amplitude on time, obtained by the numerical simulations of the equation for the normal form of Hopf bifurcation at the presence of stirring (dotted line) and absence of stirring (solid line).

the stirring effect on the Hopf equation is determined by adding a stochastic variable. Numerical simulations have shown that increasing the stirring rate increases the value of t_H as illustrated by Figure 4f. Figure 6 shows the time dependent amplitude of oscillations in the presence of stirring (dotted line) and in the absence of stirring (solid line).

Numerical simulations have shown that the stirring effect on the BZ reaction catalyzed by ferroin in a batch could not be explained in terms of stochastic noise.

6. Conclusion

The stirring effect on the BZ oscillating chemical reaction catalyzed by ferroin in a batch has been studied. The results of our work have shown that the stirring rate is a bifurcation parameter for transient regimes in the BZ oscillating chemical reaction catalyzed by ferroin in a batch. The parameters of the time-delayed Hopf bifurcation depend on the stirring rate.

The stirring effect on the BZ reaction in a batch could not be explained in the context of micromixing and macromixing concepts. To explain the experimental results and the stirring effect in general we analyzed theories of diffusion-controlled reactions and hydrodynamic turbulence. It was shown that the rate of the diffusion-controlled reaction increases if the stirring rate increases. Moreover, we have suggested a kinetic scheme that describes the experimental results. Our simulations indicate that the reaction between ferroin and BrMA• can be a diffusion-controlled reaction. It was also shown that increasing the stirring rate leads to an increasing of the rate of the reaction between ferroin and BrMA•. A good agreement between the simulations and the experimental results is obtained.

Acknowledgement

We thank Professor Z. Noszticzius for helpful discussions of the results presented in the article. The work was supported financially by the Ministry of National Education of Poland, Grant N C-31 "Hydrodynamical Effects in Complex Chemical Systems".

- [1] J.B. Marcus, M. Hauser, D. Lebender, and F.W. Schneider, *J. Phys. Chem.* **96**, 9332 (1992).
- [2] M. Menzinger and A. K. Dutt, *J. Phys. Chem.* **94**, 4510 (1990).
- [3] L. Hannon and W. Horsthemke, *J. Chem. Phys.* **86**, 140 (1987).
- [4] J. Wang, F. Hynne, P.G. Sorensen, and K. Nielsen, *J. Phys. Chem.* **100**, 17593 (1996).
- [5] A. K. Dutt, *J. Phys. Chem.* **B106**, 11069 (2002).
- [6] Z. Váradı and M. T. Beck, *J. Chem. Soc., Chem. Commun.* **30–31** (1973)
- [7] P. Sevcık and I. R. Adamčıkova, *Chem. Phys. Lett.* **146**, 419 (1988).
- [8] L. Lopez-Thomas and F. Sagues, *J. Phys. Chem.* **95**, 701 (1991).
- [9] A. K. Dutt and M. Menzinger, *J. Phys. Chem.* **96**, 8447 (1992).
- [10] P. Ruoff, *J. Phys. Chem.* **97**, 6405 (1993).
- [11] Z. Noszticzius, Z. Bodnar, L. Garamszegi, and M. Wittmann, *J. Phys. Chem.* **95**, 6575 (1991).
- [12] B. Z. Shakhshiri and J. Gordon, *J. Inorg. Chem.* **7**, 2454 (1968).
- [13] Y. Y. Kalishyn, M. Rachwalska, V. O. Khavrus, and P. E. Strizhak, *PCCP* **7**, 1680 (2005).
- [14] L. Holden and T. Erneux, *SIAM J. Appl. Math.* **53**, 1045 (1993).
- [15] F. Argoul, A. Arneodo, P. Richetti, and J. C. Roux, *J. Phys. Chem.* **86**, 3325 (1987).
- [16] P. Strizhak and M. Menzinger, *J. Chem. Phys.* **105**, 10905 (1996).
- [17] P. W. Atkins and J. de Paula, *Physical Chemistry*, 8th edition, W. H. Freeman, New York 2006.
- [18] G. Dewel, P. Borckmans, and D. Walgraef, *Phys. Rev.* **A31**, 1983 (1985).

- [19] J. A. Aronovitz and D. R. Nelson, *Phys. Rev.* **A29**, 2012 (1984).
- [20] M. M. Goncharenko, T. S. Ivashenko, V. O. Khavrus, and P. E. Strizhak, *Teoret. i Eksper. Khimiya* **34**, 153 (1998).
- [21] L. Györgyi, T. Turanyi, and R. J. Field, *J. Phys. Chem.* **94**, 7162 (1990).
- [22] M. T. M. Koper and A. Schuijff, *J. Phys. Chem.* **94**, 8135 (1990).
- [23] Y. Gao and H. D. Försterling, *J. Phys. Chem.* **99**, 8638 (1995).
- [24] S. Keki, I. Magyar, M. T. Beck, and V. Gaspar, *J. Phys. Chem* **96**, 1725 (1992).
- [25] Y.-C. Chou, H.-P. Lin, S. S. Sun, and J.-J. Jwo, *J. Phys. Chem.* **97**, 8450 (1993).
- [26] J. Wang, F. Hynne, P. G. Sorensen, and K. J. Nielsen, *J. Phys. Chem.* **100**, 17593 (1996).
- [27] L. Triendl, P. Ruoff, and P. O. Kvernberg, *J. Phys. Chem.* **101**, 4606 (1997).
- [28] D. B. Margerum, *J. Am. Chem. Soc.* **79**, 2728 (1957).